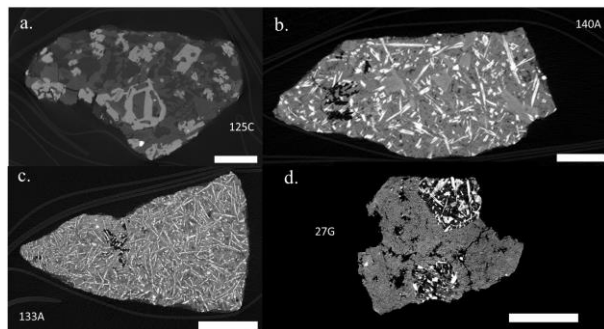


## HIGH-TI MELTS FROM THE TAURUS-LITTROW VALLEY (TLV). A PRODUCT OF VOLCANISM OR IMPACT? AN ANGSA INVESTIGATION USING THE STATION 3 DOUBLE DRIVE TUBE 73001-73002.

C.K. Shearer<sup>1,2</sup>, S.B. Simon<sup>1</sup>, C.R. Neal<sup>3</sup>, J.L. Valenciano<sup>3</sup>, S. Eckley<sup>4</sup>, B.L. Jolliff<sup>5</sup>, N. Petro<sup>6</sup> and the ANGSA Science Team<sup>7</sup>, <sup>1</sup>Dept. of Earth and Planetary Science, Institute of Meteoritics, University of New Mexico, Albuquerque, New Mexico 87131; <sup>2</sup>Lunar and Planetary Institute, Houston TX 77058; <sup>3</sup>University of Notre Dame, Notre Dame IN 46556; <sup>4</sup>ARES, NASA Johnson Space Center, Houston TX 77058-3696; <sup>5</sup>Washington University in St. Louis, St. Louis, Mo 63130; <sup>6</sup>NASA Goddard Space Flight Center, Greenbelt, MD 20771; <sup>7</sup>ANGSA Science Team list at <https://www.lpi.usra.edu/ANGSA/teams/>. (cshearer@unm.edu). (cshearer@unm.edu)

**Introduction:** The greater than 4 mm lithic fragment population in the double drive tube 73001-73002 from Station 3 is dominated by a variety of breccia (e.g., impact melt breccia, regolith breccias) [1]. There is also a variety of igneous rocks (highland, volcanics), although high-Ti basalts are the dominant igneous lithology making up the greater than 4mm size fraction. Most of the high-Ti lithologies are clearly mare basalts. However, there is a group of fine-grained, ilmenite-rich lithologies that are somewhat ambiguous with regards to their origin. To date, no unambiguous high-Ti impact melt has been observed in samples from the Moon. Figure 1 illustrates the textural transition from a clearly high-Ti mare basalt to one that is ambiguous. Are these lithologies rapidly cooled high-Ti mare basalts from margins of a lava flow, or impact melts derived from a high-Ti basalt target? Here, we examine a fairly unique high-Ti lithic fragment to better address this issue.



**Figure 1. micro-X-ray Computed Tomography (XCT) images of ilmenite-rich melt lithologies from clearly magmatic lithologies (a and b) to a fine-grained, ambiguous lithology in c. Image d illustrates a fine-grained, ilmenite-rich lithology with clasts of high-Ti basalt (see Fig. 2). Scale bars are 1 mm.**

**Analytical Strategy:** A variety of lithic fragments (>4 mm) were separated from the 73001-73002 core during Preliminary Examination (PE) of the double drive tube collected at Station 3 and imaged by micro-XCT at the NASA Johnson Space Center. The sample considered in this study is fragment 27G (73002,480). Additional fine-grained, ilmenite-bearing lithologies were allocated to other ANGSA team members. This sample was imaged

and analyzed by SEM at the University of New Mexico. Backscattered electron imaging and energy-dispersive analysis (both qualitative and quantitative) were accomplished with a TESCAN Lyra3 scanning electron microscope equipped with an IXRF silicon drift energy-dispersive X-ray detector running Iridium Ultra software. Quantitative wavelength-dispersive analyses will be obtained with a fully automated JEOL 8200 electron microprobe operated at 15kV with a focused beam, a beam current of 20 nA, calibrated with pure oxide and natural mineral standards.

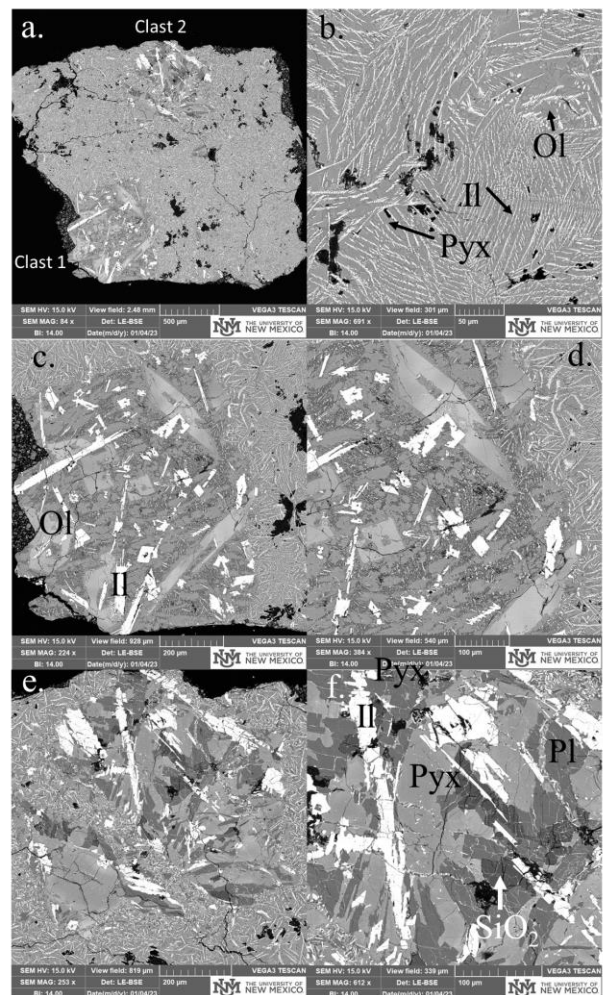


**Figure 2.** Backscattered electron (BSE) lithic fragment 27G shown in Fig. 1d. a. BSE image of 27G illustrating two distinct high-Ti basalt clasts immersed in a fine-grained ilmenite + olivine + high-Ca pyroxene melt-derived matrix. b. image of the matrix consisting of ilmenite (Il), minute, euhedral olivine (Ol), and euhedral high-Ca pyroxene. c and d. High-Ti mare basalt Clast 1 with ilmenite (Il), olivine (Ol), and high-Ca pyroxene (Pyx). e and f. High-Ti mare basalt Clast 2 with ilmenite (Il), plagioclase (Pl), pyroxene (Pyx), SiO<sub>2</sub>.

**Descriptions of textures and mineralogy:** There are three distinct lithologies associated with this lithic fragment: interclast matrix, which represents a melt; Clast 1; and Clast 2 (Figure 2a). The dominant lithology in this lithic fragment consists of an ilmenite-rich melt rock with curved, feathery dendrites of ilmenite and minute tabular crystals of olivine and pyroxene. (Figure 2b). The pyroxene is more abundant than the olivine. The olivine has a composition of Fo<sub>73</sub> and the pyroxene has an average composition of En<sub>39</sub>Wo<sub>38</sub>Fs<sub>23</sub> (Figure 3). Similar ilmenite textures in a series of experiments suggest a very rapid cooling rate for this melt (210°C/hour) [2,3]. This cooling rate is “Faster” than cooling rates determined by crystal size distributions for high-Ti mare basalt lithic fragments from 73001-73002 by Valenciano et al. [5]. There appears to have been little interaction between the clasts and the surrounding melt at their interfaces. Note the sharp clast/matrix contacts in Fig. 2c and 2d. This further suggests that the melt underwent rapid cooling. There does appear to be some penetration of the melt into the clasts. Both clasts are ilmenite basalts, but they have distinctly different mineralogies and textures. Clast 1 has early, subhedral, hopper-shaped, highly zoned olivine crystals (Fo<sub>65.5-52.9</sub>) with overgrowths of clinopyroxene (En<sub>30.7</sub>Wo<sub>49.6</sub>Fs<sub>19.7</sub> with 5.65 wt% TiO<sub>2</sub>) (Figure 3) and a quenched mesostasis (Figure 2c,d). There is little or no plagioclase. This suggests a kinetic delay in plagioclase crystallization. Clast 2 has a coarser texture, suggestive of a slower cooling rate than either the surrounding interclast matrix or clast 1 [2,3]. Its mineralogy consists of free SiO<sub>2</sub>, plagioclase, and pyroxene. There is no olivine in this clast. Plagioclase composition is An<sub>86.1</sub>. The pyroxene composition is En<sub>37.1</sub>Wo<sub>44.7</sub>Fs<sub>18.3</sub> (Figure 3). Abundant cracks in plagioclase are filled with a high-albedo material that may represent melt from the surrounding lithology.

**Conclusions:** There are several conclusions that we can reach based on these preliminary observations: (1) The rapid cooling rate clearly indicated by the texture of the host matrix implies that it is an impact-produced melt and not a product of cooling along a margin of mare basalt flow. The melt was co-saturated with ilmenite +

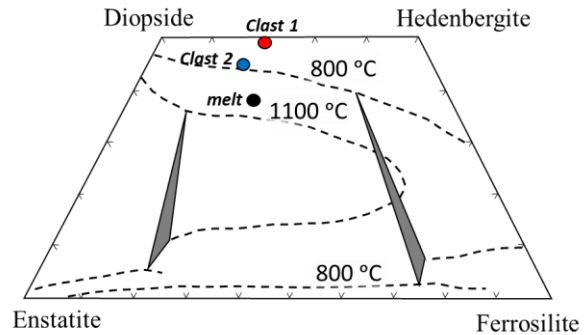


**Figure 3.** Pyroxene compositions from the three lithologies in 27G.

high-Ca pyroxene + olivine and there appears to be no individual crystals from the target material. Low pressure melting experiments of high-Ti basalt 70215 suggests near co-saturation of these phases at approximately 1150°C [5]; (2) This conclusion is further substantiated by the two clasts associated with this lithic fragment. These clasts are dramatically distinct from each other. One is olivine-normative and the other is silica-oversaturated. Still, they could potentially be crystallization products from different parts of the same flow, but pyroxene compositions suggest that they are petrologically unrelated (Figure 3). Therefore, fragment 27G is a fairly rare type of impact-melt breccia. (3) Basalt clasts in this impact-melt breccia overlap in mineralogical characteristics with other high-Ti basalts in the TLV. It appears most likely that the impact event that produced this lithic fragment occurred in the TLV and involved melting of a high-Ti basalt target, probably sampling at least two basalt units.

**Future Work:** This sample will be studied using the XCT scan data and thick section element map to construct ilmenite and potentially plagioclase and olivine CSDs to investigate the origin(s) of these samples (cf. [6]). Further, we will examine potential impact features that may be sources for these lithologies (e.g., Ching-Te).

**References:** [1] Gross J. et al. (2022) Preliminary Examination of 73001-73002. ANGSA Team webpage. [2] Usselman T. and Lofgren G. (1976) *Proc. Lunar Sci. Conf. 7<sup>th</sup>*. 1345-1363. [3] Usselman T. et al. (1975) *Proc. Lunar Sci. Conf. 6<sup>th</sup>*. 997-1020. [4] Valenciano et al. (2022) LPSC abstract #2032. [5] Longhi et al. (1974) *Proc. 5<sup>th</sup> LPSC*, 447-469. [6] Neal C.R. et al. (2015) *GCA* 148, 62-80.